ACS APPLIED MATERIALS & INTERFACES

Research Article

www.acsami.org

Polymer Composite Electrolytes Having Core–Shell Silica Fillers with Anion-Trapping Boron Moiety in the Shell Layer for All-Solid-State Lithium-Ion Batteries

Jimin Shim, Dong-Gyun Kim, Hee Joong Kim, Jin Hong Lee, and Jong-Chan Lee*

School of Chemical and Biological Engineering and Institute of Chemical Process, Seoul National University, 1 Gwanak-ro, Gwanak-gu, Seoul 151-742, Republic of Korea

Supporting Information

ABSTRACT: Core–shell silica particles with ion-conducting poly(ethylene glycol) and anion-trapping boron moiety in the shell layer were prepared to be used as fillers for polymer composite electrolytes based on organic/inorganic hybrid branched copolymer as polymer matrix for all-solid-state lithium-ion battery applications. The core–shell silica particles were found to improve mechanical strength and thermal stability of the polymer matrix and poly(ethylene glycol) and boron moiety in the shell layer increase compatibility between filler and polymer matrix. Furthermore, boron moiety in the shell layer increases both ionic conductivity and lithium transference number of the polymer matrix because lithium salt can be more easily dissociated by the anion-trapping boron. Interfacial compatibility with lithium metal anode is also improved because well-dispersed silica particles serve as protective layer against interfacial side reactions. As a result, all-solid-state battery performance was found to be enhanced when the copolymer having core–shell silica particles with the boron moiety was used as solid polymer electrolyte.

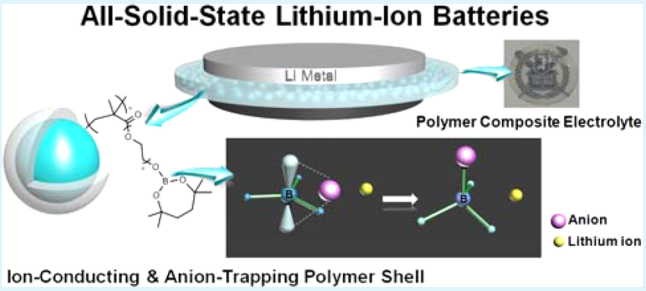

KEYWORDS: *lithium-ion battery, solid polymer electrolyte, core–shell silica, boron, lithium transference number*

INTRODUCTION

Solid polymer electrolytes (SPEs) for all-solid-state lithium-ion battery applications have been extensively studied to satisfy several requirements for next generation of energy storage and conversion devices especially related with safety issues.[1−7] Because currently used liquid electrolyte systems based on organic carbonate solvents have serious safety problems caused by leakage of liquids, their high temperature applications have been limited. On the other hand, SPEs having dimensional/thermal stability at high temperature can widen the applications of lithium-ion batteries for electrical vehicles and electricity storage systems.[2] Furthermore, lithium metal anode possessing large capacity (3860 mAh g^{-1}) can be more easily applied to the lithium battery systems using SPEs because SPE layers on the anode surface can prevent exposure of explosive lithium metal and at the same time suppress growth of lithium dendrite.[8−10] However, intrinsic low ionic conductivity originating from slow segmental motion of the solid polymer chains at ambient temperature still has to be increased for practical applications.

Among various strategies to develop the SPEs exhibiting high ionic conductivity combined with excellent mechanical stability, polymer composite electrolyte systems containing fillers such as carbon or ceramic materials have been suggested.[6,11−14] In particular, silica particles have been known as effective filler materials that can enhance both ionic conductivity and mechanical stability of the polymer electrolytes.[13−21] Furthermore, silica particle can suppress formation of irregular passivation layers at the lithium anode surface.[22,23] Because boron has an empty p-orbital that can interact with basic anion of lithium salt, chemical additives having boron moiety have been known to increase lithium transference number in the electrolyte systems; lithium transference number is defined as relative amount of the lithium-ion transport compared to that of the counteranion.[24−26] Therefore, a series of researches have been performed to prepare polymers or low-molecular-weight compounds containing boron moieties as electrolytes or additive materials to improve electrochemical properties and cycle performance of the lithium-ion batteries.[21,24,25,27−33]

Recently, organic/inorganic hybrid branched-graft copolymers (BCP) comprising poly(ethylene glycol) and polyhedral oligomeric silsesquioxane (POSS) moieties prepared in our group was reported as SPE for all-solid-state lithium-ion batteries (Scheme 1).[7] BCP was found to be promising polymer materials for the SPEs at high-temperature due to its good dimensional/thermal stability at elevated temperature. Still, ionic conductivity (1.1×10^{-5} S/cm at 30 °C) and cycle performance of the BCP need to be improved. As a continuous

Received: January 20, 2015
Accepted: March 24, 2015
Published: March 24, 2015

DOI: 10.1021/acsami.5b00618
ACS Appl. Mater. Interfaces 2015, 7, 7690−7701

Scheme 1. Synthesis of Organic/Inorganic Hybrid Branched-Graft Copolymer (BCP) via RAFT Polymerization

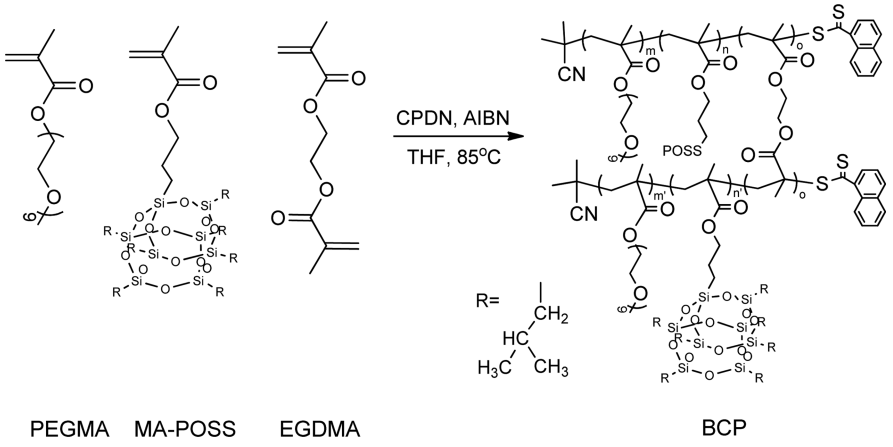

effort to improve the performance of all-solid-state lithium-ion batteries, herein, we first prepared BCP-based polymer composite electrolyte systems exhibiting high ionic conductivity and mechanical stability using core–shell silica particles having boron moiety in the shell layer as filler materials. The core–shell silica particles were found to improve mechanical stability, ionic conductivity, and transference number of the BCP matrix because of rigid silica core structures and boron moiety in the shell layers. Furthermore, excellent cycle performance was observed from the all solid-state lithium-ion battery system prepared using this polymer composite electrolyte.

EXPERIMENTAL SECTION

Chemicals and Materials. 2,2′-Azobis(isobutyronitrile) (AIBN, Junsei) was recrystallized from ethanol prior to use. Poly(ethylene glycol) methyl ether methacrylate (PEGMA, average M_n = 475 g mol^{-1}) and ethylene glycol dimethyl acrylate (EGDMA) was purchased from Aldrich and passed through an alumina column prior to polymerization. MethacrylisobutylPOSS (3-(3,5,7,9,11,13,15-heptaisobutyl-pentacyclo[9.5.1.1^{3,9}.1^{5,15}.1^{7,13}]octasiloxane-1-yl)propyl methacrylate, MA-POSS) was purchased from Hybrid Plastics (product no. MA0702) and used as received. Tetrahydrofuran (THF) was freshly distilled from sodium/benzophenone under a nitrogen atmosphere. Lithium perchlorate ($LiClO_4$, >98%, Aldrich) was dried under high vacuum at 130 °C for 24 h and subsequently placed in an argon filled glovebox. Poly(ethylene glycol) methacrylate (average M_n = 500 g mol^{-1}), 2,5-dimethylhexane-2,5-diol, trimethyl borate, tetraethyl orthosilicate (TEOS), chloro(dimethyl) vinylsilane, and 30% of ammonium hydroxide solution were purchased from Aldrich. The chain transfer agent (CTA), 2-cyanoprop-2-yl-1-dithionaphthalate (CPDN), was synthesized as previously described.[34] All the other reagents and solvents were obtained from reliable commercial sources and used as received.

Synthesis of Organic/Inorganic Hybrid Branched-Graft Copolymer (BCP). BCP comprising 21 mol % MA-POSS and 79 mol % PEGMA moiety was synthesized via reversible addition–fragmentation transfer (RAFT) polymerization as follows. PEGMA (5.0 g, 10.5 mmol), MA-POSS (2.80 g, 2.78 mmol), EGDMA (0.042 g, 0.021 mmol), CPDN (0.029 g, 0.10 mmol), and AIBN (0.006 g, 0.034 mmol) were dissolved in 12 mL of distilled THF and the solution was degassed by three repetitive freeze–pump–thaw processes to remove oxygen. Polymerization was conducted in an oil bath thermostated at 85 °C for 21 h under N_2 atmosphere. After the polymerization, unreacted monomers were removed by precipitation in *n*-hexane three times. After dried under vacuum at room temperature for 3 days, rubbery solid product was obtained with 65% of yield. ^{1}H NMR [300 MHz, $CDCl_3$, δ. (ppm), TMS ref] of BCP: 4.08 (CH_2–O–C(O)), 3.48–3.85 (CH_2–CH_2–O), 3.38 (CH_3-O), 1.85 (isobutyl, C*H*), 1.53–2.05 (methacrylate backbone, CH_2-C(CH_3)(C=O)), 0.95 (isobutyl, CH_3), 0.78–1.11 (methacrylate backbone, CH_2–C(CH_3)-(C=O)), 0.6 (isobutyl, CH_2).

Synthesis of PEGMA Containing Boronic Ester Group (B-PEGMA). 2,5-Dimethylhexane-2,5-diol (5.0 g, 0.034 mol) and trimethyl borate (3.8 mL, 0.034 mol) were dissolved in 50 mL of anhydrous acetonitrile, and the solution was stirred at 65 °C for 1 h under N_2 purging conditions. Poly(ethylene glycol) methacrylate (M_n = 500 g mol^{-1}) (12 g, 0.034 mol) was subsequently added to the solution and stirred at 65 °C for another 3 h. After the reaction, residual solvent was removed under reduced pressure by evaporation. The crude product was dissolved in toluene and cooled to room temperature. The insoluble part was removed by filtration and toluene was removed under reduced pressure at 60 °C. After being dried under vacuum at room temperature for 24 h, PEGMA containing a boronic ester group was obtained with 97% yield. The obtained product was stored in a vacuum oven to prevent contact with moisture that can hydrolyze the product. PEGMA containing boronic ester group is abbreviated as B-PEGMA. ^{1}H NMR [300 MHz, $CDCl_3$, δ (ppm), TMS ref] of B-PEGMA: 5.57–6.16 (CH_2-C(CH_3)(C=O), 2H), 3.48–3.85 (CH_2–CH_2–O, 40H), 1.97 (CH_2–C(CH_3)(C=O), 3H), 1.56 (methylene, C(CH_3)$_2$–CH_2–CH_2-C(CH_3)$_2$, 4H), 1.24 (methyl, C(CH_3)$_2$-CH_2–CH_2–C(CH_3)$_2$, 12H). Elemental anal. Found (%): C, 56.2144; H, 8.9431; O, 29.0174. Calcd for $C_{30}H_{57}O_{13}B$: C, 56.6929; H, 8.9763; O, 32.7559.

Preparation of Silica Particle Having Vinyl Group (Vinyl Si). Silica particle having average diameter of about 200 nm was prepared by StÖber method. NH_4OH (1.8 g, 0.05 mol) was dissolved in a mixed solvent (water–ethanol mixture (5:1 v/v)) and resultant solution was added to a 500 mL one-neck round bottomed flask equipped with a magnetic stirring bar. TEOS (6.3 mL, 0.028 mol) was added to the solution and then hydrolysis and condensation reactions were conducted in an oil bath thermostated at 25 °C for 1 h under N_2 atmosphere. After the flask was removed from the oil bath, unreacted TEOS was thoroughly removed by several centrifugal washing with isopropanol. Obtained silica particle was dried under high vacuum at 60 °C for 24 h. After drying, 2 g of silica particle was further reacted with 0.2 mL of chloro(dimethyl)vinylsilane in 100 mL of mixed solvent (water–ethanol mixture (5:1 v/v)) at 50 °C for 24 h. Obtained silica particle having vinyl group was dried under high vacuum at 60 °C for 24 h. For the convenience, silica particle having vinyl group is abbreviated as vinyl Si.

Preparation of Core–Shell Silica Particles (Si-P and Si-B). 0.2 g of vinyl Si was grinded and dispersed in 10 mL of distilled THF followed by ultrasonication for 30 min. 0.8 g of PEGMA and 0.04 g of AIBN were dissolved in 5 mL of distilled THF and transferred to the silica dispersed solution. The resultant solution was transferred to a 50 mL Schlenk flask equipped with a magnetic stirring bar and a condenser. The solution was degassed by three consecutive freeze–pump–thaw cycles to remove oxygen and dispersed under sonication for 30 min right before the polymerization, and then it was heated to

DOI: 10.1021/acsami.5b00618
ACS Appl. Mater. Interfaces 2015, 7, 7690–7701

70 °C for 24 h under N_2 atmosphere to convert the monomer, PEGMA, into the polymer, P(PEGMA). The unreacted monomers and free polymers unattached to the silica surface were removed by washing with THF and resultant core−shell silica particle was collected by centrifuge process. Core−shell silica particle having P(PEGMA) in the shell layer was obtained in 53% of yield after drying under high vacuum at 60 °C for 24 h. Core−shell silica particle having P(B-PEGMA) in the shell layer was also obtained in 61% of yield using same process used for the core−shell silica particle having P(PEGMA) in the shell layer except the monomer. The core−shell silica particles with P(PEGMA) in the shell layer and with P(B-PEGMA) in the shell layer are abbreviated as Si-P and Si-B, respectively.

Detachment of P(PEGMA) and P(B-PEGMA) in the Shell Layer of Si-P and Si-B. 100 mg of core−shell silica particle was dispersed in 30 mL of THF under sonication and 5 mL of hydrofluoric acid (HF) was added to the dispersed solution. Because HF is a highly corrosive chemical known as a contact poison, it was handled very carefully inside of a fume hood and stored in Teflon or polyethylene container because it even reacts with glass. The solution was stirred at room temperature for 24 h to detach the shell layer from the silica core. The resultant solution was precipitated in *n*-hexane with several times until the trace of HF was removed. Residual solvent was evaporated at reduced pressure and further dried under high vacuum at 60 °C for 24 h.

Preparation of Polymer Composite Electrolytes (BCP-vinyl Si, BCP-Si-P, and BCP-Si-B). Solid-state polymer composite electrolytes containing BCP (M_w = 16 200), $LiClO_4$, and core−shell silica fillers in various compositions were prepared by a solution casting technique. Doping levels of $LiClO_4$ are defined as a ratio of the number of lithium cations (Li^+) to that of ethylene oxide (EO) repeating unit ([Li]/[EO] = 0.07) in the polymers. 0.1 g of polymer and given amounts of $LiClO_4$ were dissolved in 0.5 mL of distilled THF and homogeneous solutions were obtained. Different amount of filler was added to the solution and stirred at room temperature for 1 day and then additionally dispersed under sonication for 30 min right before casting process. After that, the solution was cast onto a Teflon plate and dried at room temperature for 24 h. Subsequently, it was further dried under high vacuum at room temperature. Finally, film was peeled from the Teflon plate and the resultant film was placed in a high vacuum condition for a week at 60 °C prior to measure ionic conductivities. Thickness of the films measured by a micrometer (Mitutoyo, 293−330 IP 65 water resistant) was in a range of 200−230 μm. For the sake of convenience, polymer composite electrolytes having vinyl Si, Si-P, and Si-B are abbreviated as BCP-vinyl Si, BCP-Si-P, and BCP-Si-B, respectively, and the numbers after the abbreviations represent content of the fillers. For example, BCP-Si-B 10, BCP-Si-B 20, and BCP-Si-B 30 represent that they contain 10, 20, and 30 wt % Si-B, respectively.

Cell Fabrication and Electrochemical Characterization. Electrochemical stability of the polymer composite electrolytes was evaluated using linear sweep voltammetry (LSV). Cell was assembled by sandwiching electrolyte between stainless steel (working electrode) and lithium metal (reference electrode) in 2032 coin cell. The cell was swept in a potential range from 3 to 7 V (versus Li/Li^+) at a scan rate of 1 mV/s at 60 °C. Charge/discharge test of all-solid-state lithium-ion battery was performed at cutoff voltages of 2.0−3.8 V versus Li/Li^+ at 60 °C with a current density of 0.1 *C*, where a 1.0 *C* rate corresponds to a current density of 294 mAg^{-1}. V_2O_5 (70 wt %) was used as cathode active material and dispersed in *N*-methyl-2-pyrrolidone (NMP) with carbon black (20 wt %) and PVDF (10 wt %). The resultant slurry was deposited and cast onto an aluminum current collector using doctor blade. Residual NMP was completely dried under vacuum condition at 120 °C for 24 h. The obtained cathode sheet, lithium metal, and polymer composite electrolytes were punched into disks and assembled together in 2032 coin cell to form $Li/SPE/V_2O_5$ cell. All components were assembled in argon filled glovebox (H_2O < 0.5 ppm, O_2 < 0.5 ppm).

Measurement of Lithium Transference Number. Lithium transference number (T_{Li+}) was determined using DC polarization/AC impedance combination method. Polymer composite electrolyte was sandwiched between two nonblocking lithium metal disks to form a symmetrical Li/electrolyte/Li coin cell. The cell was polarized by a constant DC voltage of 10 mV and following current values were monitored until steady-state current was observed. Initial and steady-state resistances of the cell were also measured. From this method, T_{Li+} was determined by following eq 1

$$T_{Li+} = \frac{I_s(V - I_iR_i)}{I_i(V - I_sR_s)} \quad (1)$$

where V indicates a constant DC voltage applied to the cell; R_i and R_s are initial and steady-state resistances, respectively; I_i and I_s are initial and steady-state currents, respectively.

Characterization. ^1H and ^{13}C NMR spectra were recorded on an AscendTM 400 spectrometer (300 MHz) using $CDCl_3$ (Cambridge Isotope Laboratories) as a solvent at room temperature, with TMS as a reference. Solid-state ^{11}B magic angle spinning (MAS) NMR spectra were recorded on a JeolJNM-LA400 spectrometer (400 MHz) with 7 kHz MAS. Elemental analysis results were obtained with Flash 1112/2000 EA instrument (Thermo Fisher Scientific Inc., USA). Molecular weights (M_n, M_w) and polydispersity index (PDI) were analyzed by gel permeation chromatography (GPC). Relative molecular weight was measured by GPC equipped with a Waters 515 HPLC pump and three columns including PLgel 5.0 μm guard, MIXED-C and MIXED-D from Polymer Laboratories in series with a Viscotek LR125 laser refractometer. The system with a refractive index (RI) detector was calibrated using polystyrene standards from Polymer Laboratories. The resulting data was analyzed using the Omnisec software. HPLC grade THF (J. T. Baker) was used as the eluent at a flow rate of 1.0 mL min^{-1} at 35 °C. The thermal transition temperatures of the polymers were examined by differential scanning calorimetry (DSC) using TA Instruments DSC-Q1000 under a nitrogen atmosphere. Samples with a typical mass of 3−7 mg were encapsulated in sealed aluminum pans. The samples were first heated to 150 °C and then quenched to −80 °C. This was followed by a second heating scan from −80 to 150 °C at a heating rate of 10 °C min^{-1}. The thermal stability of the polymers was investigated by thermogravimetric analysis (TGA) using TA Instruments TGA Q-5000IR under nitrogen atmosphere. The samples were maintained at 130 °C for 10 min to remove residual water molecules, and then heated to 800 °C at a heating rate of 10 °C min^{-1}. FT-IR spectra were recorded in the absorption mode on Nicolet 6700 spectrophotometer with a resolution of 4 cm^{-1} in the vibrational frequency range from 400 to 4000 cm^{-1}. Field-emission scanning electron microscopy (FE-SEM) was performed on a JEOL JSM-6700F with an accelerating voltage of 10 kV. Transmission electron microscopy (TEM) was performed on a LIBRA 120 with an accelerating voltage of 120 kV. The mechanical properties were measured using a universal testing machine (LS1SC, LLOYD Instruments). The dumbbell specimens were prepared using the ASTM standard D638 (Type V specimens dog-bone shaped samples). The tensile properties of the membrane samples were measured with a gauge length and cross head speed of 15 mm and 5 mm/min, respectively. Five specimens for each sample were tested and average value was calculated. The ionic conductivity of the SPEs was analyzed by complex impedance spectroscopy between 10 and 80 °C with a Zahner Electrik IM6 apparatus in the frequency range of 0.1 Hz to 1 MHz and an applied voltage of 10 mV. The real part of the impedance at the minimum of imaginary part was used as the resistance to calculate the conductivity of the SPEs. The samples for the measurements were prepared by sandwiching the SPEs between two stainless-steel electrodes into a thickness of 200−300 μm. Each sample was allowed to equilibrate for 30 min at each temperature prior to taking measurements. The ionic conductivity (σ) was calculated from the electrolyte resistance (R) obtained from the impedance spectrum, the electrolyte thickness (d) and the area of the electrode (A) using the equation, $\sigma = (1/R)(d/A)$. Electrochemical stability was evaluated by linear sweep voltammetry (LSV) using a potentiostat (VMP3, Biologics) at 60 °C at scan rate of 1 mV/s. Charge/discharge test of all-solid-state lithium-ion battery was performed with a WBCS3000 battery cycler (WonATech) at 60 °C.

DOI: 10.1021/acsami.5b00618
ACS Appl. Mater. Interfaces 2015, 7, 7690−7701

Scheme 2. Conceptual Illustration of Polymer Composite Electrolytes Containing Core−Shell Silica Filler Having Ion-Conducting Poly(ethylene glycol) and Anion-Trapping Boron Moiety in the Shell Layer

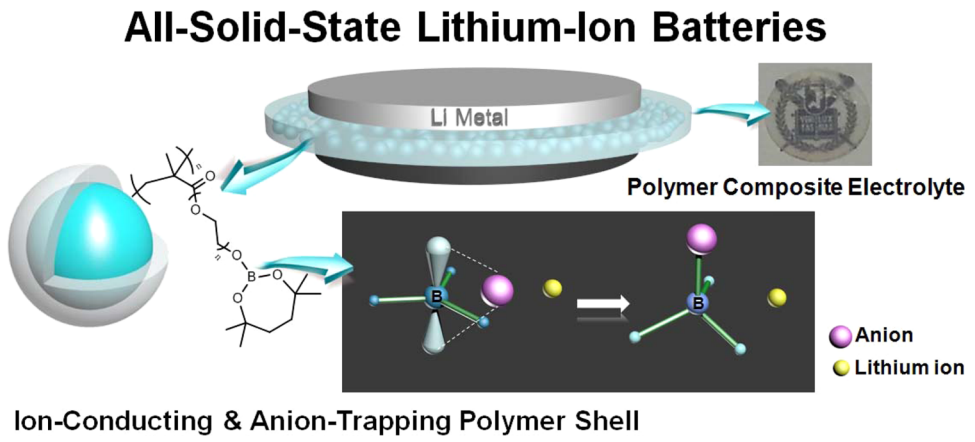

Scheme 3. Synthesis of PEGMA Containing Boronic Ester Group (B-PEGMA)

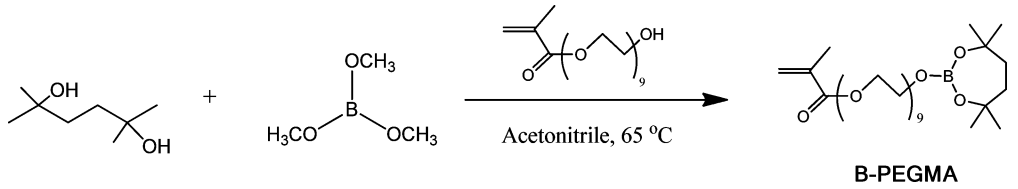

RESULT AND DISCUSSION

Synthesis and Characterization of Core−Shell Silica Particles. Core−shell silica particle having boron moiety in the shell layer was prepared to be used as filler materials to enhance ionic conductivity, lithium transference number, mechanical stability, and cycle performance of the polymer matrix, BCP, and overall concept of this study is illustrated in Scheme 2. PEGMA containing boronic ester group (B-PEGMA) was prepared to incorporate boron moiety in the shell layer of the silica particle as presented in Scheme 3. The bulky 2,5-dimethylhexyl group can increase stability of the boronic ester group from possible hydrolysis by moisture during sample preparation procedures.[35] The formation of B-PEGMA was confirmed using ^{1}H NMR analysis (Figure 1a). Proton peaks at 1.25 and 1.63 ppm (signals a and b) represent presence of alkyl and ethylene groups of the boronic ester, verifying successful incorporation of boron moiety into the PEGMA. Signals d at 3.5−4.5 ppm are assigned to ethylene oxide units and signals c, e, and f are attributed to methacrylate group of the B-PEGMA. The presence of boron moiety in the B-PEGMA was further confirmed by ^{11}B NMR analysis as shown in Figure 1b. Broad peak at about 20 ppm corresponds to characteristic signal of tricoordinate boron atoms. ^{13}C NMR and FT-IR analysis were also conducted to confirm the structure of B-PEGMA (Figure S1 and S2 in the Supporting Information, respectively).

Core−shell silica particles having P(PEGMA) and P(B-PEGMA) in the shell layers abbreviated as Si-P and Si-B, respectively, were prepared as presented in Scheme 4. Silica particle having reactive vinyl groups on surface (vinyl Si) was synthesized by hydrolysis and condensation reactions of TEOS followed by coupling reaction with chloro(dimethyl)vinylsilane. Uniform spherical shaped vinyl Si having a diameter about 200 nm was obtained and observed by SEM and TEM images as shown in Figure 2a, b, respectively. P(PEGMA) and P(B-PEGMA) can be incorporated on the shell layer of the silica particle by reaction of vinyl Si with PEGMA and B-PEGMA, respectively, in the presence of AIBN. Radical chain polymerization of the monomers, PEGMA and B-PEGMA, can produce free polymer chains (P(PEGMA) and P(B-PEGMA), respectively) unattached to the vinyl Si, while chain transfer of radical to the vinyl groups on vinyl Si can produce shell layers of P(PEGMA) and P(B-PEGMA) chains in Si-P and Si-B, respectively. The free polymers could be easily separated by washing

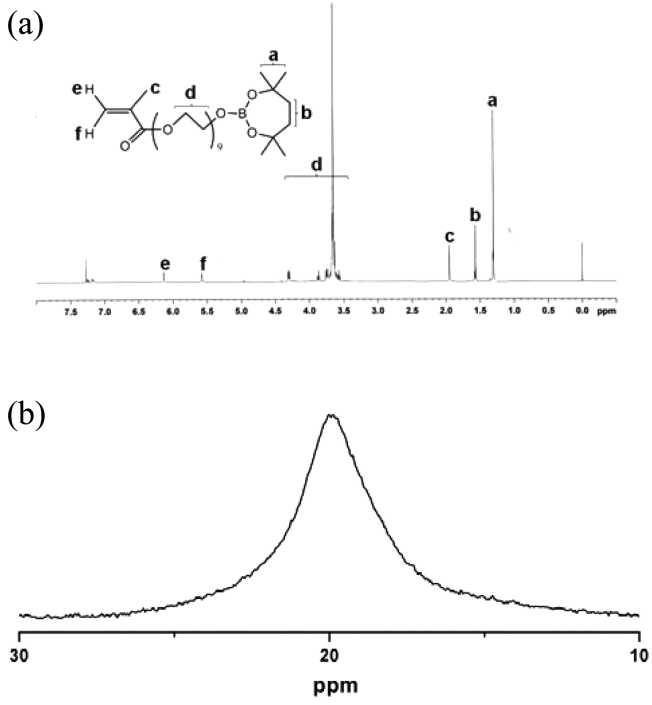

Figure 1. (a) ^{1}H NMR spectrum and (b) ^{11}B NMR spectrum of B-PEGMA.

DOI: 10.1021/acsami.5b00618
ACS Appl. Mater. Interfaces 2015, 7, 7690−7701

Scheme 4. Preparation of Core–Shell Silica Particles Having P(B-PEGMA) and P(PEGMA) in the Shell Layers Abbreviated as Si-B and Si-P, Respectively

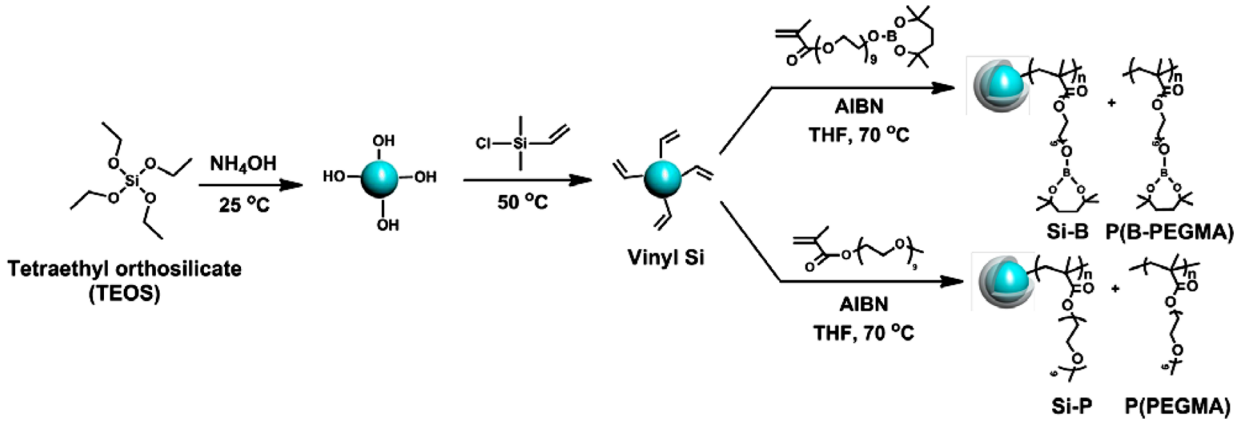

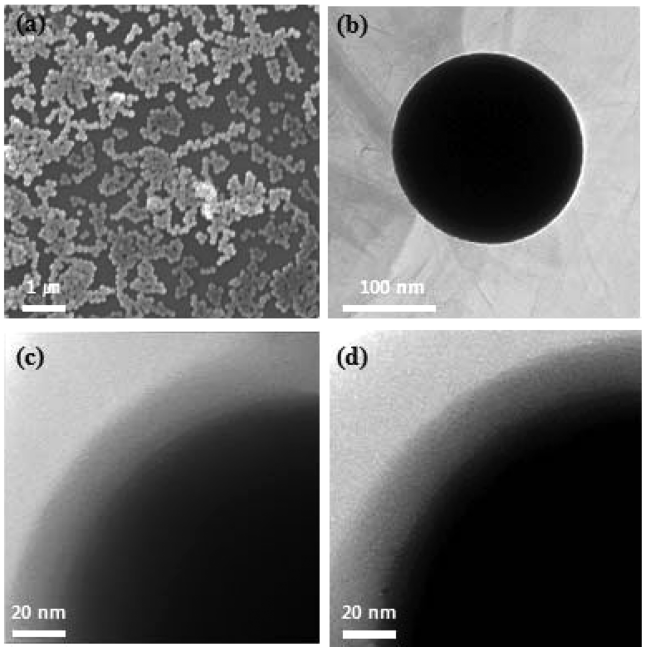

Figure 2. (a) SEM micrograph of vinyl Si and TEM micrographs of (b) vinyl Si, (c) Si-P, and (d) Si-B.

with THF (good solvent for the free polymer) and centrifuge process as described in the Experimental Section. The formation of the shell layers on Si-P and Si-B could be confirmed with TEM images and their thicknesses were found to be about 20 nm (Figure 2c, d). Characterization of vinyl Si, Si-P, and Si-B was further conducted using FT-IR analysis as shown in Figure S3 in the Supporting Information. Two IR peaks at around 1410 and 1630 cm^{-1} are attributed to vinyl groups on the vinyl Si surface. After radical chain polymerization of the monomers with vinyl Si and AIBN, intensities of vinyl peaks significantly decrease and new absorption peaks at around 1729 cm^{-1} corresponding to carbonyl groups of methacrylate group in the shell layer appear from both Si-P and Si-B, indicating successful incorporation of the polymers (P(PEGMA) and P(B-PEGMA)) from PEGMA and B-PEGMA. Furthermore, presence of boron moiety in the shell layer on Si-B was additionally confirmed with solid-state ^{11}B MAS NMR analysis; boron signal at about 20 ppm was clearly observed as shown in Figure S4 in the Supporting Information, indicating that the boronic ester group remains during polymerization and purification procedures without hydrolysis reaction, if any, because of the sterically hindered structure of 2,5-dimethylhexyl group.

The amounts of unattached free polymers and polymers attached on the shell layer could be estimated by TGA analysis for the samples obtained before and after purification process as shown in Figure S5 in the Supporting Information. TGA curves of core–shell silica particles (Si-P and Si-B) after removing the unattached free polymers by purification process show gradual weight loss with an onset temperature at around 300 °C, whereas that of the vinyl Si shows only a small change in weight. Because the residual weight at 800 °C in TGA curves have been attributed to the silica core, weight differences between vinyl Si and core–shell silica particles at 800 °C could be attributed to the amount of polymers in the shell layers.[36] The amounts of polymer shell layer on Si-P and Si-B were found to be close to about 35 wt %, indicating that the reactivity of two monomers, PEGMA and B-PEGMA, in polymerization is very close. The weight differences between the TGA curves at 800 °C before and after purification process could be attributed to the amounts of unattached free polymers,[37] and they were found to be 39 and 44 wt % for the free P(B-PEGMA) and free P(PEGMA), respectively.

The molecular weights of detached polymers from Si-P and Si-B by etching process using HF solution were measured by GPC and they were found to be 8500 for P(B-PEGMA) from Si-B and 7900 for P(PEGMA) from Si-P, respectively. The molecular weights of unattached free polymers were found to be 12 300 and 11 700 for free P(B-PEGMA) and P(PEGMA), respectively. The smaller molecular weight of detached polymers from Si-B and Si-P than those of free polymers could be ascribed to steric effect; radicals on the silica surface should be much more sterically hindered than those in the free polymer chains and then they become less reactive.[38]

Preparation of Polymer Composite Electrolytes (BCP-vinyl Si, BCP-Si-P, and BCP-Si-B). Polymer composite electrolytes containing different amounts of vinyl Si, Si-P, and Si-B were prepared to study the effects of silica cores and shell layers on various physicochemical and electrochemical properties of the SPEs. Free-standing films of the polymer composite electrolytes containing various filler contents (10, 20, and 30 wt %) (Figure 3) could be easily prepared and their transparent and/or translucent states indicate that the fillers are more or less well-dispersed in the polymer matrix without much aggregation. Furthermore, all the electrolytes are flexible and

DOI: 10.1021/acsami.5b00618
ACS Appl. Mater. Interfaces 2015, 7, 7690–7701

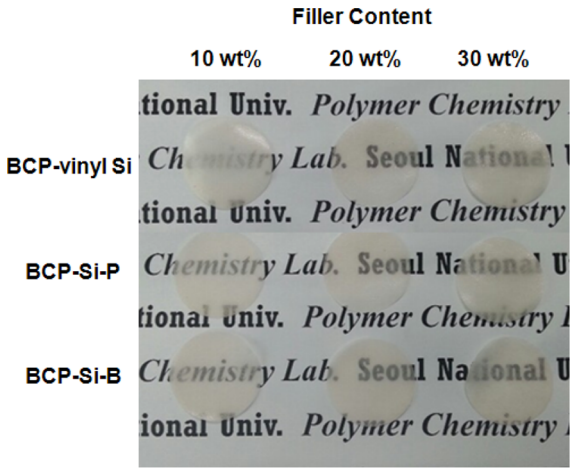

Figure 3. Photographs of polymer composite electrolytes (BCP-vinyl Si, BCP-Si-P, and BCP-Si-B) having different amount of vinyl Si, Si-P, and Si-B containing $LiClO_4$ ([Li]/[EO] = 0.07).

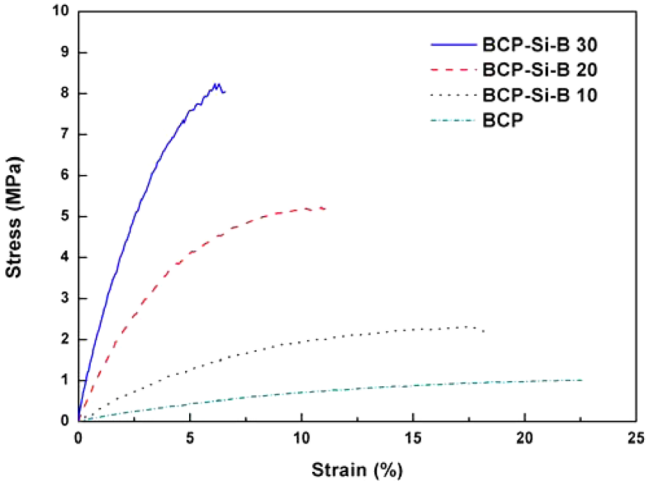

Figure 4. Stress–strain curves of BCP and BCP-Si-B having different amounts of Si-B, where BCP-Si-B 10, BCP-Si-B 20, and BCP-Si-B 30 represent contents of 10, 20, and 30 wt % Si-B, respectively.

physically stable. When the polymer composite electrolytes were prepared using larger filler content than 30 wt %, electrolyte films became quite opaque and brittle, indicating that the fillers are aggregated forming large separated domains. Therefore, 30 wt % of filler content was decided to be the maximum content for preparation of the polymer composite electrolytes. $LiClO_4$ was chosen as a lithium salt for the preparation of polymer composite electrolytes because boron has been known to be more strongly interacted with hard Lewis basic anions such as $CF_3SO_3^-$ and ClO_4^- than soft basic anions such as $N(CF_3SO_2)_2^-$.[39] The concentration of $LiClO_4$ was fixed as [Li]/[EO] = 0.07 based on our previous studies on pure polymer electrolyte systems using the polymer matrix materials, BCP, used in this study; maximum ionic conductivity was observed at this concentration.[6,7] SEM image of BCP-vinyl Si 30 shows aggregated particles, whereas those of BCP-Si-P 30 and BCP-Si-B 30 show well-dispersed particles, as shown in Figure S6 in the Supporting Information. Therefore, core–shell silica particles (Si-P and Si-B) are much more compatible with the polymer matrix than vinyl Si without the shell layers. Obviously, shell layers comprising P(PEGMA) or P(B-PEGMA) can increase compatibility between fillers and polymer matrix because PEGMA units in the polymer matrix, BCP, can well-interact with the same ethylene oxide units in the shell layers on Si-P and Si-B. On the contrary, BCP is not compatible with more or less hydrophobic vinyl Si having vinyl groups on the surface.[36,40] In polymer composite electrolyte systems, it is very desirable for the fillers to be well-dispersed because aggregated filler domains can act as barriers to prevent ion transport.[6,41]

Mechanical and Electrochemical Stability of Polymer Composite Electrolytes. Mechanical reinforcement effect of the core–shell silica fillers was studied by measuring mechanical properties such as Young's modulus, tensile strength, and elongation at break from stress–strain curves as presented in Figure 4 and these values are listed in Table 1. It was found that incorporation of core–shell silica fillers (Si-P and Si-B) increases both Young's modulus and tensile strength of the electrolytes, which is attributed to reinforcement effect of rigid inorganic silica core well-dispersed in the polymer matrix. For example, 30 wt % Si-P increases Young's modulus and tensile strength by 23 and 7 times, respectively, and 30 wt % Si-B increases them by 25 and 8 times, respectively, compared with

Table 1. Mechanical Properties of BCP and Polymer Composite Electrolytes (BCP-Si-B and BCP-Si-P) Having Different Amounts of Filler

	filler content (wt %)	Young's modulus (MPa)	tensile strength (MPa)	elongation at break (%)
BCP	0	12.23 ± 1.1	1.01 ± 0.1	22.8 ± 1.3
BCP-vinyl Si		N/A[a]		
BCP-Si-B 10	10	39.20 ± 0.2	2.32 ± 0.1	18.2 ± 0.6
BCP-Si-B 20	20	154.7 ± 0.7	5.27 ± 0.2	11.4 ± 0.2
BCP-Si-B 30	30	302.6 ± 2.4	8.24 ± 0.4	6.59 ± 0.5
BCP-Si-P 10	10	40.43 ± 1.2	1.20 ± 0.2	20.1 ± 1.2
BCP-Si-P 20	20	127.9 ± 0.8	5.82 ± 0.4	13.4 ± 1.4
BCP-Si-P 30	30	281.5 ± 1.9	7.15 ± 0.5	7.19 ± 0.9

[a]The mechanical properties of BCP-vinyl Si samples could not be obtained because they are too brittle.

those of polymer matrix, BCP. The percentage of elongation at break was found to decrease with the increase of filler contents. Similar increases in mechanical strength and decrease in flexibility have been reported by other groups.[42−44] Mechanical properties of BCP-vinyl Si could not be obtained because dog-bone samples are too brittle to maintain their shapes during the measurement in testing equipment. Because hydrophobic vinyl Si particles are aggregated in the polymer matrix (see Figure S6a in the Supporting Information), the electrolytes are not physically stable.[42] Therefore, it is worthy to note that P(PEGMA) and P(B-PEGMA) in the shell layers increase compatibility with BCP, and then mechanically stable polymer composite electrolytes could be obtained.

The incorporation of core–shell silica fillers was found to improve thermal/dimensional stability of the polymer matrix, BCP. When the BCP was heated to 100 °C, it shrank to smaller size and converted to a waxy state within 2 min, because T_g values of P(PEGMA) segments and POSS moiety in BCP are below 100 °C like about −67 and 76 °C, respectively.[7] In contrast, when BCP-Si-B having different amount of Si-B were heated to 100 °C, all the electrolytes maintain their shapes, sizes, and solid-state even after several days at 100 °C, indicating that these polymer composite electrolytes could be used for high-temperature applications. The photographs of

DOI: 10.1021/acsami.5b00618
ACS Appl. Mater. Interfaces 2015, 7, 7690−7701

electrolytes at 25 and 100 °C are presented in Figure S7 in the Supporting Information.

Electrochemical stability of polymer composite electrolytes was evaluated using linear sweep voltammetry. Figure 5 shows

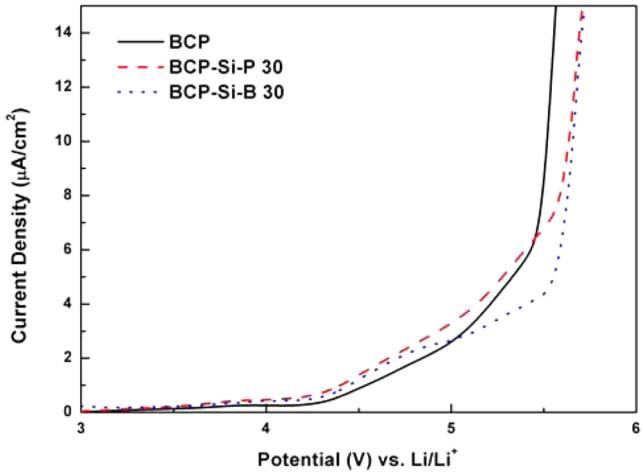

Figure 5. Linear sweep voltammogram of BCP and polymer composite electrolytes having 30 wt % Si-P and Si-B (BCP-Si-P 30 and BCP-Si-B 30) at 60 °C with a scan rate of 1 mV/s.

linear sweep voltammogram of BCP, BCP-Si-P 30, and BCP-Si-B 30 having the maximum filler content, 30 wt %. The abrupt rise in current corresponding to decomposition of electrolyte limits operation voltage range of electrodes. It was revealed that BCP, BCP-Si-P, and BCP-Si-B exhibit wide electrochemically stable window (~4.3 V), indicating that these electrolytes are not degraded within a voltage range of 4 V class cathode materials.

Ion Transport Properties. Figure 6 shows ionic conductivities of polymer composite electrolytes containing different

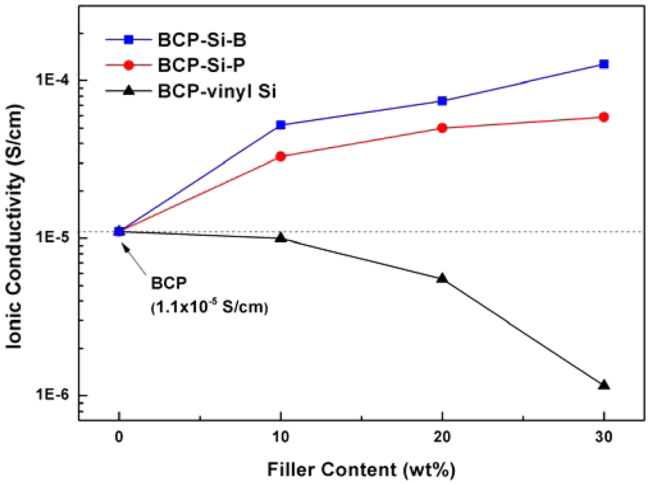

Figure 6. Ionic conductivities of polymer composite electrolytes (BCP-Si-B, BCP-Si-P, and BCP-vinyl Si) having different amounts of filler at 30 °C.

filler contents (10, 20, and 30 wt %) at 30 °C. Ionic conductivity of polymer composite electrolytes having filler contents larger than 30 wt % could not be measured because they are not mechanically stable as described previously. When the core–shell silica fillers (Si-P and Si-B) were introduced, ionic conductivity continuously increases with the filler content up to 30 wt %. On the contrary, ionic conductivity of the polymer composite electrolyte having vinyl Si without any shell layers continuously decreases with the filler content due to poor dispersion state of hydrophobic vinyl Si which disturbs the ion conduction.[14,16] Furthermore, the incorporation of vinyl Si dilutes the concentration of ion-conducting ethylene oxide units in the polymer composite electrolytes, resulting in decrease of ionic conductivity, whereas both Si-P and Si-B do not decrease that much because they have additional ion-conducting polymer shell. Interestingly, this ionic conductivity behavior is consistent with trends in free anion (ClO_4^-) fraction (Figure 7). The free anion fraction was calculated using

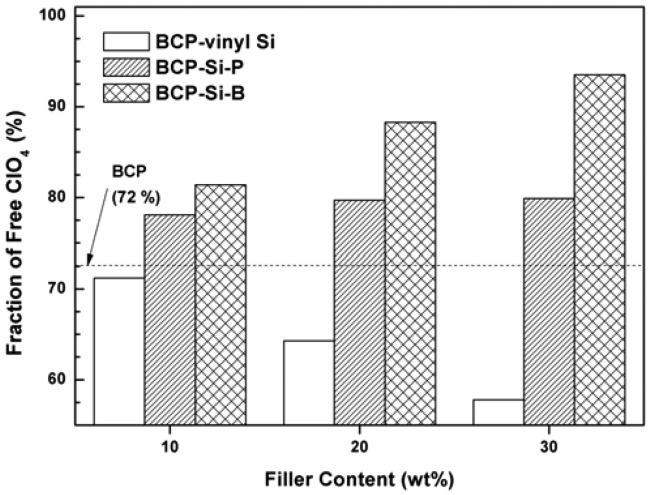

Figure 7. Fractions of free ClO_4^- anion of polymer composite electrolytes (BCP-vinyl Si, BCP-Si-P, and BCP-Si-B) having different amounts of filler.

FT-IR analysis method.[30] Thus, the more free ions in the electrolyte system, the larger the ionic conductivity. When vinyl Si was used as filler, free anion fraction was found to be even smaller than that of the BCP without any filler, and it decreases with the increase in filler content. Obviously, aggregated hydrophobic vinyl Si fillers in the polymer matrix decrease interfacial area of fillers interacting with lithium salts and serve as a barrier disturbing the ion transport.[45] Free anion fraction values of BCP-Si-B are larger than those of BCP-Si-P or BCP-vinyl Si, indicating that boron moiety in Si-B effectively increases the amount of dissociated lithium salt, because boron moiety can trap the anion.[46] Furthermore, increases in Si-B content further increase the free anion fraction values, whereas in increase in Si-P does not increase the free anion fraction value much. Still, the free anion fraction values of BCP-Si-P are larger than those of BCP because free volume can be increased by the incorporation of silica fillers in well-dispersed state.[41,47] Because the number and mobility of both cation and anion can affect the ionic conductivity, one might claim that Si-B can decrease the ionic conductivity because it traps the anion, thereby decreasing the mobility of the anion. Still, ionic conductivities of BCP-Si-B are larger than those of BCP-Si-P, possibly because the increase in number of dissociated free lithium cation can positively offset the decrease in anion mobility by boron moiety.

The anion-trapping effect of boron moiety in BCP-Si-B could be figured out by observing glass transition temperature (T_g) behaviors of P(PEGMA) and P(B-PEGMA) detached from

DOI: 10.1021/acsami.5b00618
ACS Appl. Mater. Interfaces 2015, 7, 7690–7701

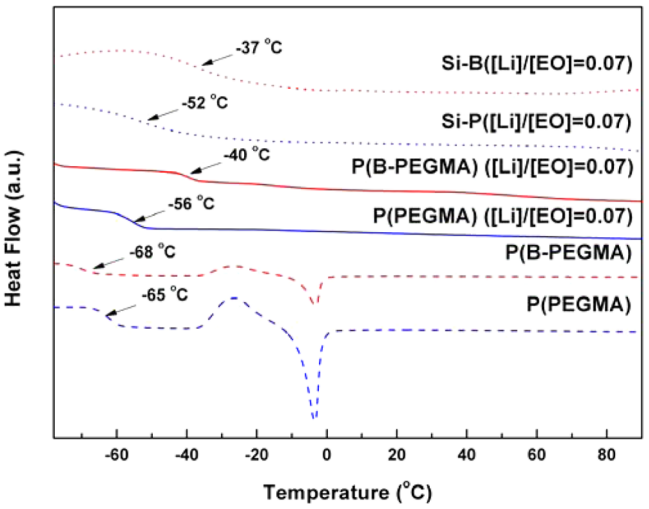

Figure 8. DSC thermogram of detached P(B-PEGMA) and P(PEGMA); with and without $LiClO_4$ and core−shell silica fillers; Si-P and Si-B with $LiClO_4$.

Si-P and Si-B by HF etching process. Figure 8 shows glass transition temperatures (T_g) of detached P(PEGMA) and P(B-PEGMA) with and without lithium salt and core−shell silica fillers; Si-P and Si-B having lithium salt. Although the T_g values of detached P(PEGMA) and P(B-PEGMA) without any lithium salt are quite close as observed at −65 and −68 °C, respectively, their melting transition peaks are observed at same temperature (−4 °C) by side chain crystals formed by same ethylene oxide units in the side chains of polymers. The slightly smaller T_g value of P(B-PEGMA) than that of P(PEGMA) could be ascribed to the bulky boronic ester group that can easily increase free volume of the polymers, resulting in decreasing the T_g.[7,48,49] When lithium salt ([Li]/[EO] = 0.07) is added to the polymers, melting transition peaks disappear because lithium salt can suppress the crystallization of the side chains.[50] T_gs of both P(B-PEGMA) and P(PEGMA) are increased by the addition of lithium salt because pseudocross-linked structures formed by interactions between ethylene oxide units and lithium cation can decrease chain mobility.[51] Furthermore, T_g values of detached P(B-PEGMA) (−40 °C) and attached P(B-PEGMA) on the Si-B (−37 °C) are quite larger than those of the detached P(PEGMA) (−56 °C) and attached P(PEGMA) on the Si-P (−52 °C), respectively. The larger T_g values of the polymer chains attached on the silica particles than those of the detached polymer chains are because the polymer chains on the silica particles are less mobile than the corresponding free polymer chains.[52] The larger T_g values of P(B-PEGMA) having $LiClO_4$ than those of P(PEGMA) can be ascribed to the decrease in the chain mobility because larger amount of lithium salts are dissociated in the P(B-PEGMA) due to the anion-trapping boron moiety. It has been generally reported that polymers having larger amounts of lithium salt exhibit larger T_g value because lithium cation can act as a transient cross-linking agent.[53] In addition, interaction between boron moiety in P(B-PEGMA) and anion of lithium salt by acid−base interaction can also decrease the chain mobility.

Although the chain mobility of ion-conducting segments decreases with the incorporation of boron moiety in the shell layer, ionic conductivity of BCP-Si-B is still larger than that of BCP-Si-P because large amount of charge carriers by boron moiety can offset the decrease in chain mobility. It is also well-known that filler particles can provide additional ion-conducting pathway to facilitate the ion transport by increasing the free volume of the polymer matrix.[41,54,55]

To evaluate the anion-trapping effect of boron moiety quantitatively, we measured lithium transference numbers (T_{Li+}) of the polymer composite electrolytes using DC polarization/AC impedance combination method (Figure 9).[56] T_{Li+} of BCP-Si-B

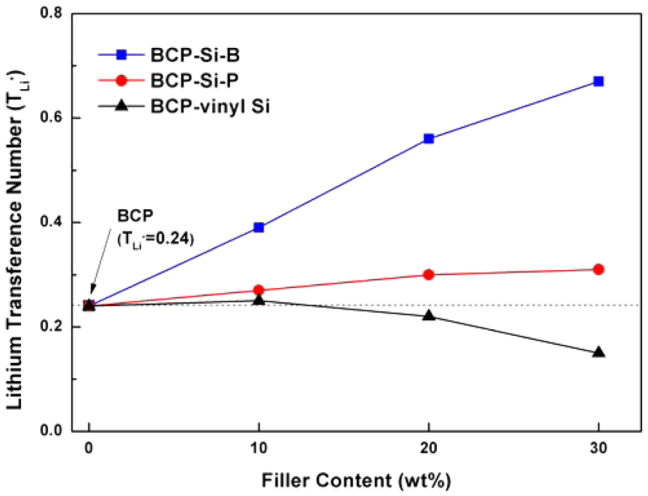

Figure 9. Lithium transference numbers of polymer composite electrolytes (BCP-Si-B, BCP-Si-P, and BCP-vinyl Si) having different amounts of filler at 60 °C.

linearly increases with the filler content and maximum T_{Li+} value of 0.67 was observed for BCP-Si-B 30. T_{Li+} of BCP-Si-P also increases with the filler content, whereas the increase is much less compared to that of BCP-Si-B. Therefore, boron moiety in Si-B can more effectively trap the anion of the lithium salt than the pure ethylene oxide moiety in Si-P, resulting in larger T_{Li+} values. T_{Li+} values of BCP-vinyl Si were found to even decrease with the filler content. Because vinyl Si particles are poorly dispersed in the polymer matrix, BCP, they probably act as barriers for ion transport. Furthermore, aggregation of filler decreases interfacial area interacting with the lithium salt, resulting in smaller dissociation of the lithium salt.[40,45] For the same reasons, BCP-vinyl Si show smaller ionic conductivity value than those of BCP-Si-B and BCP-Si-P. This kind of behavior has been reported by other groups.[45,57] In our case, Si-P and Si-B can increase both T_{Li+} and ionic conductivity because they are compatible with the polymer matrix and also increase dissociation of the lithium salt.

The effect of lithium salt on the ion transport properties was also investigated using other lithium salts such as $LiCF_3SO_3$ and LiTFSI (Figure S8 in the Supporting Information). It was found that ionic conductivity and transference number values of BCP-Si-B 30 having $LiClO_4$ and $LiCF_3SO_3$ are larger than those of BCP-Si-B 30 having LiTFSI because boron can interact with hard Lewis basic anions such as $CF_3SO_3^-$ and ClO_4^- more strongly than soft basic anions such as $N(CF_3SO_2)_2^-$.[39] Comparing $CF_3SO_3^-$ and ClO_4^-, the polymer composite electrolyte having $LiClO_4$ shows slightly larger values than that having LiTFSI.

Because Si-B is a very effective filler material for improving the electrochemical properties of BCP because of the anion-trapping ability of the boron moiety, P(B-PEGMA) itself without the silica core part can also improve those properties. However, when about 10 wt % P(B-PEGMA) was mixed with

DOI: 10.1021/acsami.5b00618
ACS Appl. Mater. Interfaces 2015, 7, 7690−7701

BCP, the resulting mixture turned into a wax state because P(B-PEGMA) has a very low T_g value as shown in Figure 8. Because the main objective of this study is to develop a novel solid polymer electrolyte system for all-solid-state lithium-ion batteries, we did not try to prepare the polymer electrolytes using P(B-PEGMA). The effect of the boron moiety for the electrolytes in liquid or wax state was already reported by others before.[24,27,29−32]

Interfacial Compatibility and Cycle Performance. Because lithium metal easily reacts with any kind of compounds in electrolytes including oxygen and residual solvents, passivating solid electrolyte interphase (SEI) layers are inevitably formed at the interface between lithium metal anodes and electrolytes, resulting in increase of interfacial resistance.[58,59] Although the SEI layers can suppress further possible side reactions between lithium and impurities, they can also increase interfacial resistance against efficient charge transport and accelerate growth of lithium dendrites, especially when they have irregular structures.[60−62] Inorganic filler materials such as silica, zeolite, and metal organic framework (MOF) have been known to suppress formation of irregular passivating layer effectively by decreasing exposed surface area of the lithium metal interacting with the electrolyte.[22,23,63,64] Furthermore, silica particles have been known to suppress the interfacial side reactions because they can trap organic impurities including solvents by interactions between the organic impurities and polar groups on silica surface.[23]

Interfacial resistances of polymer composite electrolytes were measured using symmetrically assembled Li/electrolyte/Li coin cells stored under open-circuit condition at 60 °C for 50 days to estimate the formation of SEI layers and compatibility of the electrolytes with the lithium metal anode. As shown in Figure 10, interfacial resistance of BCP without filler increases

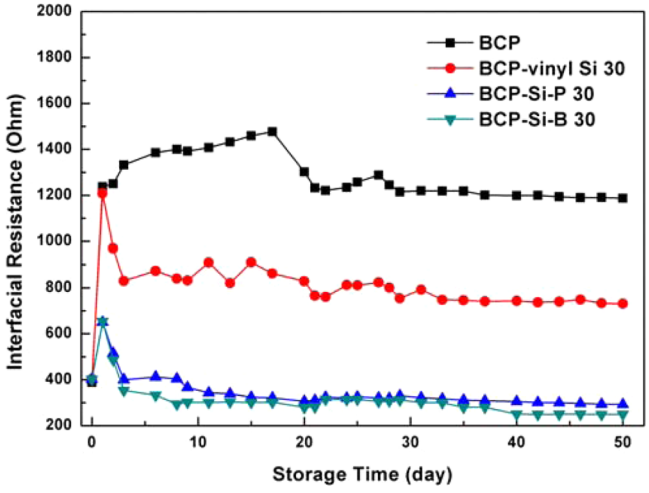

Figure 10. Interfacial resistances of symmetrically assembled Li/electrolyte/Li coin cells stored under open-circuit condition at 60 °C as a function of storage time, where BCP and the polymer composite electrolytes having 30 wt % filler (BCP-vinyl Si 30, BCP-Si-P 30, and BCP-Si-B 30) were used as electrolytes.

rapidly with storage time and their resistance values are much larger than those of polymer composite electrolytes having fillers. Therefore, it can be concluded that stable interfacial SEI layers are formed at the lithium metal surface for the polymer composite electrolytes having fillers. Although the interfacial resistance values of BCP-vinyl Si are smaller than that of BCP, they are still larger than those of BCP-Si-P and BCP-Si-B; poorly dispersed vinyl Si particles cannot effectively suppress the increase of interfacial resistance. It was further revealed that an increase in Si-B content from 10 to 30 wt % decreases interfacial resistances (see Figure S9 in the Supporting Information), indicating that a larger amount of compatible Si-B fillers can more effectively decrease the exposed surface area of lithium metal and side reactions.

Figure 11 shows cycle performance of all-solid-state batteries assembled with Li/SPEs/V_2O_5, where SPEs are BCP, BCP-Si-P

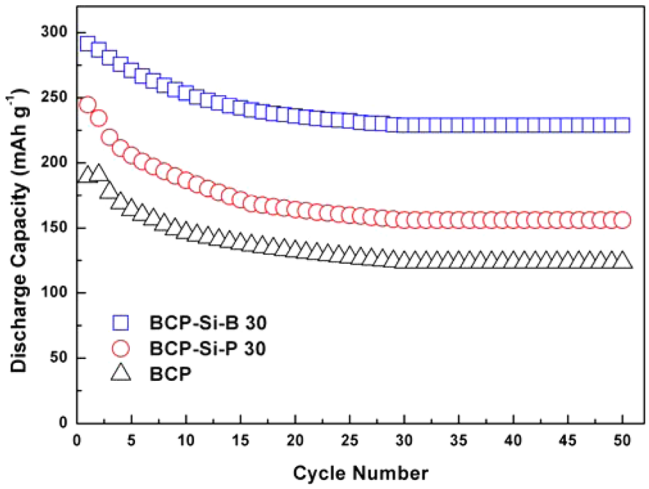

Figure 11. Discharge capacity profiles of all-solid-state Li/SPEs/V_2O_5 cell cycled at 60 °C with a scan rate of 0.1 *C*, where the SPEs are BCP and the polymer composite electrolytes containing 30 wt % of fillers (BCP-Si-B 30 and BCP-Si-P 30).

30, and BCP-Si-B 30, respectively. Filler content was fixed as 30 wt % because the maximum ionic conductivities were observed at this concentration. Liquid electrolytes have been known to be not stable at high temperature due to their volatility and flammability, resulting in serious safety problems.[65] In contrast, our SPEs show stable cycle behavior at 60 °C for 50 cycles. The initial capacity value of BCP-Si-B 30 is 291 mAh g^{-1}, which is very close to the theoretical capacity of V_2O_5, and BCP-Si-B exhibited larger capacity and retention values than those of BCP or BCP-Si-P due to the larger ionic conductivity, anion-trapping effect of boron moiety, and smaller interfacial resistance. As a result, BCP-Si-B 30 shows large capacity value and retention (80%) than BCP and BCP-Si-P 30; the retentions of BCP and BCP-Si-P 30 are 65 and 64%, respectively. Therefore, it was clearly demonstrated that the incorporation of boron moiety in the SPEs remarkably increases both capacity and retention. Further works to study the cycle performance on rate property, cycle reversibility, and high-temperature condition over 60 °C are under progress.

CONCLUSION

In this study, core−shell silica particles with ion-conducting poly(ethylene glycol) and anion-trapping boron moiety in the shell layer were prepared and used as filler materials of polymer composite electrolytes for all-solid-state lithium-ion battery applications. Mechanical strength and thermal stability of the polymer matrix were increased by incorporating core−shell silica particle into the polymer matrix. Furthermore, dimensional stability of the polymer composite electrolytes maintained even at elevated temperature up to 100 °C,

DOI: 10.1021/acsami.5b00618
ACS Appl. Mater. Interfaces 2015, 7, 7690−7701

suggesting possible applications for high-temperature batteries. Maximum ionic conductivity of 1.6×10^{-4} S/cm at 30 °C was achieved when 30 wt % of core−shell silica particle having boron moiety in the shell layer was incorporated and this value is 1 order of magnitude higher than that of the polymer matrix because boron moiety effectively traps anion of lithium salt, thereby increasing the amount of dissociated lithium ion. Moreover, excellent interfacial compatibility between polymer composite electrolytes and lithium metal anode was observed since well-dispersed fillers act as protective layer on lithium surface by suppressing possible interfacial side reactions. All of these electrochemical advantages of polymer composite electrolytes contribute to obtain excellent cycle performance at high temperature, 60 °C.

■ ASSOCIATED CONTENT

Supporting Information

Additional tables and figures: ^{13}C NMR of PEGMA and B-PEGMA (Figure S1); IR spectra of B-PEGMA and other reactants (Figure S2); IR spectra of vinyl Si, Si-P, and Si-B (Figure S3); solid-state ^{11}B MAS NMR of Si-B (Figure S4); TGA profiles of vinyl Si, Si-B, and Si-P (before and after purification process) (Figure S5); SEM images of BCP-vinyl Si 30, BCP-Si-P 30, and BCP-Si-B 30 (Figure S6); photographs of BCP and BCP-Si-B having different filler contents at 25 and 100 °C (Figure S7); ionic conductivity and lithium transference number of BCP-Si-B 30 containing different lithium salts (Figure S8); and interfacial resistances of symmetrically assembled Li/BCP-Si-B/Li coin cells stored under open-circuit condition at 60 °C as a function of storage time (Figure S9). This material is available free of charge via the Internet at http://pubs.acs.org.

■ AUTHOR INFORMATION

Corresponding Author

*E-mail: jongchan@snu.ac.kr. Phone: +82 2 880 7070. Fax: +82 2 888 1604.

Notes

The authors declare no competing financial interest.

■ ACKNOWLEDGMENTS

This research was supported by the Technology Innovation Program (Grant 10045221) funded by the Ministry of Trade, Industry and Energy (MOTIE, Korea).

■ REFERENCES

(1) Tarascon, J. M.; Armand, M. Issues and Challenges Facing Rechargeable Lithium Batteries. *Nature* **2001**, *414*, 359−367.

(2) Meyer, W. H. Polymer Electrolytes for Lithium-Ion Batteries. *Adv. Mater.* **1998**, *10*, 439−448.

(3) Kim, D. G.; Shim, J. M.; Lee, J. H.; Kwon, S. J.; Baik, J. H.; Lee, J. C. Preparation of Solid-State Composite Electrolytes Based on Organic/Inorganic Hybrid Star-Shaped Polymer and PEG-Functionalized POSS for All-Solid-State Lithium Battery Applications. *Polymer* **2013**, *54*, 5812−5820.

(4) Kim, D. G.; Sohn, H. S.; Kim, S. K.; Lee, A.; Lee, J. C. Star-Shaped Polymers Having Side Chain POSS Groups for Solid Polymer Electrolytes; Synthesis, Thermal Behavior, Dimensional Stability, and Ionic Conductivity. *J. Polym. Sci., Part A: Polym. Chem.* **2012**, *50*, 3618−3627.

(5) Kim, S. K.; Kim, D. G.; Lee, A.; Sohn, H. S.; Wie, J. J.; Nguyen, N. A.; Mackay, M. E.; Lee, J. C. Organic/Inorganic Hybrid Block Copolymer Electrolytes with Nanoscale Ion-Conducting Channels for Lithium Ion Batteries. *Macromolecules* **2012**, *45*, 9347−9356.

(6) Shim, J.; Kim, D. G.; Kim, H. J.; Lee, J. H.; Baik, J. H.; Lee, J. C. Novel Composite Polymer Electrolytes Containing Poly(ethylene glycol)-Grafted Graphene Oxide for All-Solid-State Lithium-Ion Battery Applications. *J. Mater. Chem. A* **2014**, *2*, 13873−13883.

(7) Shim, J.; Kim, D.-G.; Lee, J. H.; Baik, J. H.; Lee, J.-C. Synthesis and Properties of Organic/Inorganic Hybrid Branched-Graft Copolymers and Their Application to Solid-State Electrolytes for High-Temperature Lithium-Ion Batteries. *Polym. Chem.* **2014**, *5*, 3432−3442.

(8) Khurana, R.; Schaefer, J. L.; Archer, L. A.; Coates, G. W. Suppression of Lithium Dendrite Growth Using Cross-Linked Polyethylene/Poly(ethylene oxide) Electrolytes: A New Approach for Practical Lithium-Metal Polymer Batteries. *J. Am. Chem. Soc.* **2014**, *136*, 7395−7402.

(9) Kim, S. H.; Choi, K. H.; Cho, S. J.; Kil, E. H.; Lee, S. Y. Mechanically Compliant and Lithium Dendrite Growth-Suppressing Composite Polymer Electrolytes for Flexible Lithium-Ion Batteries. *J. Mater. Chem. A* **2013**, *1*, 4949−4955.

(10) Liu, S.; Imanishi, N.; Zhang, T.; Hirano, A.; Takeda, Y.; Yamamoto, O.; Yang, J. Lithium Dendrite Formation in Li/Poly(ethylene oxide)-Lithium Bis(trifluoromethanesulfonyl)imide and N-Methyl-N-propylpiperidinium Bis(trifluoromethanesulfonyl)-imide/Li Cells. *J. Electrochem. Soc.* **2010**, *157*, A1092−A1098.

(11) Zhou, D.; Mei, X. G.; Ouyang, J. Y. Ionic Conductivity Enhancement of Polyethylene Oxide-LiClO4 Electrolyte by Adding Functionalized Multi-Walled Carbon Nanotubes. *J. Phys. Chem. C* **2011**, *115*, 16688−16694.

(12) Tang, C. Y.; Hackenberg, K.; Fu, Q.; Ajayan, P. M.; Ardebili, H. High Ion Conducting Polymer Nanocomposite Electrolytes Using Hybrid Nanofillers. *Nano Lett.* **2012**, *12*, 1152−1156.

(13) Ju, S. H.; Lee, Y. S.; Sun, Y. K.; Kim, D. W. Unique Core-Shell Structured $SiO_2(Li^+)$ Nanoparticles for High-Performance Composite Polymer Electrolytes. *J. Mater. Chem. A* **2013**, *1*, 395−401.

(14) Hu, X. L.; Hou, G. M.; Zhang, M. Q.; Rong, M. Z.; Ruan, W. H.; Giannelis, E. P. A New Nanocomposite Polymer Electrolyte Based on Poly(vinyl alcohol) Incorporating Hypergrafted Nano-Silica. *J. Mater. Chem.* **2012**, *22*, 18961−18967.

(15) Lee, Y. S.; Ju, S. H.; Kim, J. H.; Hwang, S. S.; Choi, J. M.; Sun, Y. K.; Kim, H.; Scrosati, B.; Kim, D. W. Composite Gel Polymer Electrolytes Containing Core-Shell Structured $SiO_2(Li^+)$ Particles for Lithium-Ion Polymer Batteries. *Electrochem. Commun.* **2012**, *17*, 18−21.

(16) Chen-Yang, Y. W.; Wang, Y. L.; Chen, Y. T.; Li, Y. K.; Chen, H. C.; Chiu, H. Y. Influence of Silica Aerogel on the Properties of Polyethylene Oxide-Based Nanocomposite Polymer Electrolytes for Lithium Battery. *J. Power Sources* **2008**, *182*, 340−348.

(17) Jeddi, K.; Sarikhani, K.; Qazvini, N. T.; Chen, P. Stabilizing Lithium/Sulfur Batteries by a Composite Polymer Electrolyte Containing Mesoporous Silica Particles. *J. Power Sources* **2014**, *245*, 656−662.

(18) Jia, Z.; Yuan, W.; Zhao, H.; Hu, H. Y.; Baker, G. L. Composite Electrolytes Comprised of Poly(ethylene oxide) and Silica Nanoparticles with Grafted Poly(ethylene oxide)-Containing Polymers. *RSC Adv.* **2014**, *4*, 41087−41098.

(19) Nugent, J. L.; Moganty, S. S.; Archer, L. A. Nanoscale Organic Hybrid Electrolytes. *Adv. Mater.* **2010**, *22*, 3677−3680.

(20) Lu, Y. Y.; Moganty, S. S.; Schaefer, J. L.; Archer, L. A. Ionic Liquid-Nanoparticle Hybrid Electrolytes. *J. Mater. Chem.* **2012**, *22*, 4066−4072.

(21) Schaefer, J. L.; Yanga, D. A.; Archer, L. A. High Lithium Transference Number Electrolytes via Creation of 3-Dimensional, Charged, Nanoporous Networks from Dense Functionalized Nanoparticle Composites. *Chem. Mater.* **2013**, *25*, 834−839.

(22) Liu, S.; Imanishi, N.; Zhang, T.; Hirano, A.; Takeda, Y.; Yamamoto, O.; Yang, J. Effect of Nano-Silica Filler in Polymer Electrolyte on Li Dendrite Formation in Li/Poly(ethylene oxide)-$Li(CF_3SO_2)_2N$/Li. *J. Power Sources* **2010**, *195*, 6847−6853.

(23) Walls, H. J.; Zhou, J.; Yerian, J. A.; Fedkiw, P. S.; Khan, S. A.; Stowe, M. K.; Baker, G. L. Fumed Silica-Based Composite Polymer

DOI: 10.1021/acsami.5b00618
ACS Appl. Mater. Interfaces 2015, 7, 7690−7701

Electrolytes: Synthesis, Rheology, and Electrochemistry. *J. Power Sources* **2000**, *89*, 156−162.
(24) Lee, H. S.; Yang, X. Q.; Xiang, C. L.; McBreen, J.; Choi, L. S. The Synthesis of a New Family of Boron-Based Anion Receptors and the Study of Their Effect on Ion Pair Dissociation and Conductivity of Lithium Salts in Nonaqueous Solutions. *J. Electrochem. Soc.* **1998**, *145*, 2813−2818.
(25) Kurono, R.; Mehta, M. A.; Inoue, T.; Fujinami, T. Preparation and Characterization of Lithium Ion Conducting Borosiloxane Polymer Electrolytes. *Electrochim. Acta* **2001**, *47*, 483−487.
(26) Jakle, F. Lewis Acidic Organoboron Polymers. *Coord. Chem. Rev.* **2006**, *250*, 1107−1121.
(27) Mizumo, T.; Sakamoto, K.; Matsumi, N.; Ohno, H. Simple Introduction of Anion Trapping Site to Polymer Electrolytes Through Dehydrocoupling or Hydroboration Reaction Using 9-Borabicyclo[3.3.1]nonane. *Electrochim. Acta* **2005**, *50*, 3928−3933.
(28) Mathews, K. L.; Budgin, A. M.; Beeram, S.; Joenathan, A. T.; Stein, B. D.; Werner-Zwanziger, U.; Pink, M.; Baker, L. A.; Mahmoud, W. E.; Carini, J. P.; Bronstein, L. M. Solid Polymer Electrolytes Which Contain Tricoordinate Boron for Enhanced Conductivity and Transference Numbers. *J. Mater. Chem. A* **2013**, *1*, 1108−1116.
(29) Li, L. F.; Lee, H. S.; Li, H.; Yang, X. Q.; Huang, X. J. A Pentafluorophenylboron Oxalate Additive in Non-Aqueous Electrolytes for Lithium Batteries. *Electrochem. Commun.* **2009**, *11*, 2296−2299.
(30) Lee, Y. M.; Seo, J. E.; Choi, N. S.; Park, J. K. Influence of Tris(pentafluorophenyl) Borane as an Anion Receptor on Ionic Conductivity of $LiClO_4$-Based Electrolyte for Lithium Batteries. *Electrochim. Acta* **2005**, *50*, 2843−2848.
(31) Choi, N. S.; Ryu, S. W.; Park, J. K. Effect of Tris(methoxy diethylene glycol) Borate on Ionic Conductivity and Electrochemical Stability of Ethylene Carbonate-Based Electrolyte. *Electrochim. Acta* **2008**, *53*, 6575−6579.
(32) Choi, N. S.; Lee, Y. M.; Cho, K. Y.; Ko, D. H.; Park, J. K. Protective Layer with Oligo(ethylene glycol) Borate Anion Receptor for Lithium Metal Electrode Stabilization. *Electrochem. Commun.* **2004**, *6*, 1238−1242.
(33) Chakrabarti, A.; Filler, R.; Mandal, B. K. Borate Ester Plasticizer for PEO-Based Solid Polymer Electrolytes. *J. Solid State Electrochem.* **2008**, *12*, 269−272.
(34) Benaglia, M.; Rizzardo, E.; Alberti, A.; Guerra, M. Searching for More Effective Agents and Conditions for the RAFT Polymerization of MMA: Influence of Dithioester Substituents, Solvent, and Temperature. *Macromolecules* **2005**, *38*, 3129−3140.
(35) Kuivila, H. G.; Keough, A. H.; Soboczenski, E. J. Areneboronates from Diols and Polyols. *J. Org. Chem.* **1954**, *19*, 780−783.
(36) Zhu, L. J.; Zhu, L. P.; Zhao, Y. F.; Zhu, B. K.; Xu, Y. Y. Anti-Fouling and Anti-Bacterial Polyethersulfone Membranes Quaternized from the Additive of Poly(2-dimethylamino ethyl methacrylate) Grafted SiO_2 Nanoparticles. *J. Mater. Chem. A* **2014**, *2*, 15566−15574.
(37) Borase, T.; Iacono, M.; Ali, S. I.; Thornton, P. D.; Heise, A. Polypeptide Core-Shell Silica Nanoparticles with High Grafting Density by N-Carboxyanhydride (NCA) Ring Opening Polymerization as Responsive Materials and for Bioconjugation. *Polym. Chem.* **2012**, *3*, 1267−1275.
(38) Shin, H.; Nguyen, C.; Kim, B.; Han, M.; Kim, J. S.; Kim, J. Synthesis and Characteristics of Acrylol Borate as New Acrylic Gelator for Lithium Secondary Battery. *Macromol. Res.* **2008**, *16*, 134−481.
(39) Bailly, B.; Donnenwirth, A. C.; Bartholome, C.; Beyou, E.; Bourgeat-Lami, E. Silica-Polystyrene Nanocomposite Particles Synthesized by Nitroxide-Mediated Polymerization and Their Encapsulation Through Miniemulsion Polymerization. *J. Nanomater.* **2006**, *76371*, 1−10.
(40) Kato, Y.; Suwa, K.; Ikuta, H.; Uchimoto, Y.; Wakihara, M.; Yokoyama, S.; Yabe, T.; Yamamoto, M. Influence of Lewis Acidic Borate Ester Groups on Lithium Ionic Conduction in Polymer Electrolytes. *J. Mater. Chem.* **2003**, *13*, 280−285.
(41) Xu, L. X.; Xu, F.; Chen, F.; Yang, J. T.; Zhong, M. Q. Improvement in Comprehensive Properties of Poly(methyl methacrylate)-Based Gel Polymer Electrolyte by a Core-Shell Poly(methyl methacrylate)-Grafted Ordered Mesoporous Silica. *J. Nanomater.* **2012**, *457967*, 1−10.
(42) Ji, K. S.; Moon, H. S.; Kim, J. W.; Park, J. W. Role of Functional Nano-Sized Inorganic Fillers in Poly(Ethylene Oxide)-Based Polymer Electrolytes. *J. Power Sources* **2003**, *117*, 124−130.
(43) Li, Q.; Wood, E.; Ardebili, H. Elucidating the Mechanisms of Ion Conductivity Enhancement in Polymer Nanocomposite Electrolytes for Lithium Ion Batteries. *Appl. Phys. Lett.* **2013**, *102*, 243903.
(44) Ishibe, S.; Anzai, K.; Nakamura, J.; Konosu, Y.; Ashizawa, M.; Matsumoto, H.; Tominaga, Y. Ion-Conductive and Mechanical Properties of Polyether/Silica Thin Fiber Composite Electrolytes. *React. Funct. Polym.* **2014**, *81*, 40−44.
(45) Wang, Q.; Song, W. L.; Fan, L. Z.; Shi, Q. Effect of Alumina on Triethylene Glycol Diacetate-2-Propenoic Acid Butyl Ester Composite Polymer Electrolytes for Flexible Lithium Ion Batteries. *J. Power Sources* **2015**, *279*, 405−412.
(46) Merkel, T. C.; Freeman, B. D.; Spontak, R. J.; He, Z.; Pinnau, I.; Meakin, P.; Hill, A. J. Sorption, Transport, and Structural Evidence for Enhanced Free Volume in Poly(4-Methyl-2-Pentyne)/Fumed Silica Nanocomposite Membranes. *Chem. Mater.* **2003**, *15*, 109−123.
(47) Ryu, H.-S.; Kim, D.-G.; Lee, J.-C. Synthesis and Properties of Polysiloxanes Containing Polyhedral Oligomeric Silsesquioxane (POSS) and Oligo (ethylene oxide) Groups in the Side Chains. *Macromol. Res.* **2010**, *18*, 1021−1029.
(48) Ryu, H.-S.; Kim, D.-G.; Lee, J.-C. Polysiloxanes Containing Polyhedral Oligomeric Silsesquioxane Groups in the Side Chains; Synthesis and Properties. *Polymer* **2010**, *51*, 2296−2304.
(49) Singh, T. J.; Bhat, S. V. Morphology and Conductivity Studies of a New Solid Polymer Electrolyte: $(PEG)_xLiClO_4$. *Bull. Mater. Sci.* **2003**, *26*, 707−714.
(50) Tominaga, Y.; Takizawa, N.; Ohno, H. Effect of Added Salt Species on the Ionic Conductivity of PEO/Sulfonamide Salt Hybrids. *Electrochim. Acta* **2000**, *45*, 1285−1289.
(51) Savin, D. A.; Pyun, J.; Patterson, G. D.; Kowalewski, T.; Matyjaszewski, K. Synthesis and Characterization of Silica-Graft-Polystyrene Hybrid Nanoparticles: Effect of Constraint on the Glass-Transition Temperature of Spherical Polymer Brushes. *J. Polym. Sci., Part A: Polym. Phys.* **2002**, *40*, 2667−2676.
(52) Wu, F.; Feng, T.; Bai, Y.; Wu, C.; Ye, L.; Feng, Z. G. Preparation and Characterization of Solid Polymer Electrolytes Based on PHEMO and PVDF-HFP. *Solid State Ionics* **2009**, *180*, 677−680.
(53) Itoh, T.; Mitsuda, Y.; Ebina, T.; Uno, T.; Kubo, M. Solid Polymer Electrolytes Composed of Polyanionic Lithium Salts and Polyethers. *J. Power Sources* **2009**, *189*, 531−535.
(54) Sun, X.; Lee, H. S.; Yang, X. Q.; McBreen, J. Comparative Studies of the Electrochemical and Thermal Stability of Two Types of Composite Lithium Battery Electrolytes Using Boron-Based Anion Receptors. *J. Electrochem. Soc.* **1999**, *146*, 3655−3659.
(55) Bruce, P. G.; Evans, J.; Vincent, C. A. Conductivity and Transference Number Measurements on Polymer Electrolytes. *Solid State Ionics* **1988**, *28*, 918−922.
(56) Kim, S.; Park, S. J. Preparation and Electrochemical Behaviors of Polymeric Composite Electrolytes Containing Mesoporous Silicate Fillers. *Electrochim. Acta* **2007**, *52*, 3477−3484.
(57) Younesi, R.; Hahlin, M.; Roberts, M.; Edstrom, K. The SEI Layer Formed on Lithium Metal in the Presence of Oxygen: A Seldom Considered Component in the Development of the Li-O_2 Battery. *J. Power Sources* **2013**, *225*, 40−45.
(58) Lewandowski, A.; Swiderska-Mocek, A.; Waliszewski, L. Solid Electrolyte Interphase Formation on Metallic Lithium. *J. Solid State Electrochem.* **2012**, *16*, 3391−3397.
(59) Choi, S. M.; Kang, I. S.; Sun, Y. K.; Song, J. H.; Chung, S. M.; Kim, D. W. Cycling Characteristics of Lithium Metal Batteries Assembled with a Surface Modified Lithium Electrode. *J. Power Sources* **2013**, *244*, 363−368.
(60) Lee, S. H.; Harding, J. R.; Liu, D. S.; D'Arcy, J. M.; Shao-Horn, Y.; Hammond, P. T. Li-Anode Protective Layers for Li Rechargeable

DOI: 10.1021/acsami.5b00618
ACS Appl. Mater. Interfaces 2015, 7, 7690−7701

Batteries via Layer-by-Layer Approaches. *Chem. Mater.* **2014**, *26*, 2579−2585.
(61) Ding, F.; Xu, W.; Graff, G. L.; Zhang, J.; Sushko, M. L.; Chen, X. L.; Shao, Y. Y.; Engelhard, M. H.; Nie, Z. M.; Xiao, J.; Liu, X. J.; Sushko, P. V.; Liu, J.; Zhang, J. G. Dendrite-Free Lithium Deposition via Self-Healing Electrostatic Shield Mechanism. *J. Am. Chem. Soc.* **2013**, *135*, 4450−4456.
(62) C Gerbaldi, C.; Nair, J. R.; Kulandainathan, M. A.; Kumar, R. S.; Ferrara, C.; Mustarelli, P.; Stephan, A. M. Innovative High Performing Metal Organic Framework (MOF)-Laden Nanocomposite Polymer Electrolytes for All-Solid-State Lithium Batteries. *J. Mater. Chem. A* **2014**, *2*, 9948−9954.
(63) Xi, J. Y.; Qiu, X. P.; Cui, M. Z.; Tang, X. Z.; Zhu, W. T.; Chen, L. Q. Enhanced Electrochemical Properties of PEO-Based Composite Polymer Electrolyte with Shape-Selective Molecular Sieves. *J. Power Sources* **2006**, *156*, 581−588.
(64) Qiu, W. L.; Ma, X. H.; Yang, Q. H.; Fu, Y. B.; Zong, X. F. Novel Preparation of Nanocomposite Polymer Electrolyte and Its Application to Lithium Polymer Batteries. *J. Power Sources* **2004**, *138*, 245−252.
(65) Murata, K.; Izuchi, S.; Yoshihisa, Y. An Overview of the Research and Development of Solid Polymer Electrolyte Batteries. *Electrochim. Acta* **2000**, *45*, 1501−1508.

DOI: 10.1021/acsami.5b00618
ACS Appl. Mater. Interfaces 2015, 7, 7690−7701